G3, 2023, 13(6), jkad073
https://doi.org/10.1093/g3journal/jkad073
Advance Access Publication Date: 1 April 2023
Genome Report

A happy accident: a novel turfgrass reference genome

Alyssa R. Phillips,[1,*,†] Arun S. Seetharam,[2,†] Patrice S. Albert,[3] Taylor AuBuchon-Elder,[4] James A. Birchler,[3] Edward S. Buckler,[5,6,7] Lynn J. Gillespie,[8] Matthew B. Hufford,[3] Victor Llaca,[9] Maria Cinta Romay,[6] Robert J. Soreng,[10] Elizabeth A. Kellogg,[4] Jeffrey Ross-Ibarra[1,11,*]

[1]Department of Evolution and Ecology and Center for Population Biology, University of California, Davis, CA 95616, USA
[2]Department of Ecology, Evolution, and Organismal Biology, Iowa State University, Ames, IA 50011, USA
[3]Division of Biological Sciences, University of Missouri, Columbia, MO 65201, USA
[4]Donald Danforth Plant Science Center, Olivette, MO 63132, USA
[5]School of Integrative Plant Sciences, Section of Plant Breeding and Genetics, Cornell University, Ithaca, NY 14850, USA
[6]Institute for Genomic Diversity, Cornell University, Ithaca, NY 14850, USA
[7]Agricultural Research Service, United States Department of Agriculture, Ithaca, NY 14850, USA
[8]Botany Section, Research and Collections, Canadian Museum of Nature, Ottawa, ON K2P 2R1, Canada
[9]Corteva Agriscience, Johnston, IA 50131, USA
[10]Deptartment of Botany, Smithsonian Institution, Washington, DC 20560, USA
[11]Genome Center, University of California, Davis, CA 95616, USA

Corresponding author: Department of Evolution and Ecology and Center for Population Biology, University of California, Davis, CA 95616, USA. Email: arphillips@ucdavis.edu; Corresponding author: Department of Evolution and Ecology and Center for Population Biology, University of California, Davis, CA 95616, USA; Genome Center, University of California, Davis, CA 95616, USA. Email: rossibarra@ucdavis.edu
[†]Co-first authors.

Abstract

Poa pratensis, commonly known as Kentucky bluegrass, is a popular cool-season grass species used as turf in lawns and recreation areas globally. Despite its substantial economic value, a reference genome had not previously been assembled due to the genome's relatively large size and biological complexity that includes apomixis, polyploidy, and interspecific hybridization. We report here a fortuitous de novo assembly and annotation of a *P. pratensis* genome. Instead of sequencing the genome of a C4 grass, we accidentally sampled and sequenced tissue from a weedy *P. pratensis* whose stolon was intertwined with that of the C4 grass. The draft assembly consists of 6.09 Gbp with an N50 scaffold length of 65.1 Mbp, and a total of 118 scaffolds, generated using PacBio long reads and Bionano optical map technology. We annotated 256K gene models and found 58% of the genome to be composed of transposable elements. To demonstrate the applicability of the reference genome, we evaluated population structure and estimated genetic diversity in *P. pratensis* collected from three North American prairies, two in Manitoba, Canada and one in Colorado, USA. Our results support previous studies that found high genetic diversity and population structure within the species. The reference genome and annotation will be an important resource for turfgrass breeding and study of bluegrasses.

Keywords: Poaceae, genome assembly, aneuploidy, polyploidy, genetic diversity, population structure, Kentucky bluegrass, turfgrass

Introduction

Poa pratensis L., commonly known as Kentucky bluegrass, is an economically valuable horticultural crop grown globally on lawns and recreational areas as turf (Haydu *et al.* 2006). Native to Europe and Asia, it was introduced to North America in the seventeenth century by European colonizers as a forage crop (Carrier and Bort 1916; Raggi *et al.* 2015). Today, Kentucky bluegrass is the most popular cool-season grass used for turf due to its vigorous growth and quick establishment that creates a dense, strong sod with a long lifespan (Casler and Duncan 2003).

Today, there are 40 million acres of managed turf in the United States, an area approximately the size of the state of Florida (Milesi *et al.* 2005). While this massive area has the potential to serve as an important carbon sink, the large water and fertilization resources required currently outweigh the benefits (Milesi *et al.* 2005). Breeding efforts are underway to improve environmental-stress tolerances, disease and insect resistance, seed quality and yield, as well as uniformity and stability of traits (reviewed in Bonos and Huff 2013). While the economic value of *P. pratensis* is high, it is highly invasive, and in the last 30 years it has aggressively invaded the North American Northern Great Plains, altering ecosystem function by reducing pollinator and plant diversity and altering nutrient dynamics (DeKeyser *et al.* 2015; Kral-O'Brien *et al.* 2019; Hendrickson *et al.* 2021). Continued research into the genetic diversity of wild *P. pratensis* is needed to understand how invasive populations are rapidly adapting, and the study of wild populations may enable identification of disease or environmentally tolerant ecotypes for use in turfgrass breeding.

Previous studies using random amplified polymorphic DNA (RAPD), inter simple sequence repeats (ISSR), and microsatellites markers demonstrated high genetic diversity in both developed cultivars and wild populations but limited population structure

Received: March 08, 2022. **Accepted:** March 19, 2023

between these groups (Honig *et al.* 2012; Bushman *et al.* 2013; Raggi *et al.* 2015; Honig *et al.* 2018, but see Dennhardt *et al.* 2016). Population divergence has been detected amongst some wild populations (Dennhardt *et al.* 2016) but the extent of population structure is unclear. There are a number of potential reasons for finding a lack of population structure, including gene flow, the independent development of cultivated lines from locally adapted ecotypes (Bonos and Huff 2013; Raggi *et al.* 2015), and geographic heterogeneity in patterns of genetic diversity. Repeated reversion of cultivars to wild forms has also been suggested, but is unlikely (Dennhardt *et al.* 2016). Alternatively, previous studies may simply not have had sufficient marker resolution to detect population structure in a highly heterozygous polyploid species like *P. pratensis*.

Genetic analysis and improvement of turfgrass are challenging because of apomixis and polyploidy (Bushman and Warnke 2013). *P. pratensis* is a facultative apomict, meaning it can reproduce sexually or asexually by aposporous apomixis, and it is a polyploid with frequent aneuploidy (Brown 1939). Although apomixis is a highly valued trait for seed production, high rates of apomixis stymie the recombination needed to genetically analyze traits or recombine beneficial traits into one cultivar (Bonos and Huff 2013). Polyploidy and aneuploidy further these difficulties due to copy number variation of regions of interest and non-Mendelian inheritance resulting from double reduction. While some progress has been made in managing apomixis (Funk and Sang 1967; Pepin and Funk 1971; Matzk 1991), including the discovery of its genetic basis (Albertini *et al.* 2004; Marconi *et al.* 2020), the development of additional molecular and genomic tools in *P. pratensis* are needed to move genetic analysis and breeding efforts forward in the face of its complex biology.

Here, we report the first *P. pratensis* genome. While attempting to assemble the genome for a C4 prairie grass, *Andropogon gerardi*, we unknowingly sequenced and assembled a wild *Poa* growing in the same pot. Fortunately, this resulted in a highly contiguous, near complete genome assembly. We utilized the reference genome and wild *Poa* from three prairies to investigate the genetic diversity and population structure of North American *Poa*. The reference genome and annotation presented here are an important advancement for Kentucky bluegrass breeding. Additionally, this reference genome provides an important resource for the study of closely related bluegrasses including *P. trivialis* L., *P. annua* L., and *P. arachnifera* Torr.

Materials and methods

Sample collection

Rhizomes of *Poa* species were collected fortuitously as part of a different project aimed at collecting major C4 prairie grasses (*A. gerardi* Vitman, *Sorghastrum nutans* (L.) Nash, and *Schizachyrium scoparium* (Michx.) Nash) in moist prairies in Colorado, USA and two prairies in Manitoba, Canada (Supplementary Table S1). Necessary permissions and permits were obtained prior to collecting. Plants were brought back to the United States from Canada under phytosanitary certificate #3193417.

The C4 focal plants were dug up with a shovel late in the growing season in 2018 (when the *Poa* was dormant and thus invisible), soil was washed off, rhizomes were wrapped in wet paper towels, and leaves were cut back to about 4 in. height to reduce transpiration. The focal C4 plant was placed in a 1-gallon Ziploc bag and returned to the plant growth facility at the Donald Danforth Plant Science Center in St. Louis, MO, USA. Plants were potted in 2:1 BRK20 promix soil to turface. The previously dormant *Poa* plants produced fresh green leaves in this setting and grew faster than the C4 plant with which it was entwined. Once it was discovered that *Poa* had interpolated itself into the rhizome and root area of the C4 plants, the *Poa* plants were extricated and placed in separate pots.

One *Poa* was found inside the pot for an *A. gerardi* genotype which was used to attempt assembly of a reference genome. Instead of collecting tissue from the *A. gerardi* plant, tissue was accidentally sampled from the *Poa* plant. This *Poa* individual is referred to as the *Poa* reference individual (Supplementary Table S1). Eight additional *Poa*, referred to here as the *Poa* population panel, were discovered in various pots for C4 grasses whose genomes we attempted to sequence.

As *Poa* species generally require vernalization to flower, several plants were over-wintered outside under mulch and flowered in spring 2020 and/or 2021; voucher specimens were taken from these plants to verify species identity and have been deposited at the Smithsonian Institution (Washington, District of Columbia, USA) and the Missouri Botanical Garden (St. Louis, MO, USA.) (Heide 1994). Not all *Poa* individuals survived, so some specimens lack vouchers. Additionally, not all surviving *Poa* flowered, so vegetative vouchers were submitted (Supplementary Table S1).

PacBio sequencing

Approximately 4.1 g fresh tissue from the reference individual was extracted for PacBio sequencing using a high molecular weight DNA approach based on the Circulomics Big DNA Kit (Circulomics, USA). This method yields DNA with a center of mass at 200 Kb, which is sufficient to construct PacBio CLR 20 Kb + libraries. Sequencing was completed on the Sequel II across four SMRTCells. DNA extraction and sequencing were completed by Corteva Agriscience.

Bionano optical map generation

DNA was extracted from 0.7 g of fresh leaf tissue from the reference individual using agarose embedded nuclei and the Bionano Prep Plant Tissue DNA Isolation kit. DNA extraction, labeling, imaging, and optical map assembly followed the methods previously described in Hufford *et al.* (2021) and was completed by Corteva Agriscience.

Preparation and imaging of metaphase spreads

Metaphase spreads were utilized to estimate chromosome count and ploidy of the reference individual. Root tips were harvested from a recent off-shoot of the reference individual, treated with nitrous oxide (3 h at 160 psi) to stop mitosis in metaphase (Kato 1999), then processed as previously described in Kato *et al.* (2004, 2011) with minor modification. Specifically, the root tips were fixed in 90% acetic acid for 15 min, then rinsed with and stored in 70% ethanol at −20 °C. Ethanol was removed from the root tips prior to enzymatic digestion by soaking in water for 10 min. About 1 mm of the tip (meristem and root cap) was excised and transferred to a tube containing 20 μL of 3% cellulase R-10 (Desert Biologicals, Phoenix, AZ) and 1.25% pectolyase Y-23 (Desert Biologicals) in citrate buffer (10 mM sodium citrate, 10 mM EDTA, adjusted to pH 5.5 with citric acid) on ice. The tissue was digested for approximately 1 h at 37 °C. Seventy percent ethanol was used to inactivate the enzymes and rinse the samples. The ethanol was replaced with approximately 7 μL of a solution of 90% acetic acid and 10% methanol. The tissue was broken and cells dispersed using a blunted dissecting probe. The entire volume

was dropped from a height less than 1 cm onto a microscope slide in a container lined with wet paper towels and allowed to dry.

Preparations were counterstained with a 1/20 dilution of Vectashield with DAPI (Vector Laboratories, Burlingame, CA). Images were captured using Applied Spectral Imaging software (Carlsbad, CA) on an Olympus BX 61 fluorescence microscope. Photoshop Brightness/Contrast and Curves functions were used to decrease background noise and better define the chromosomal arms.

Genome size estimation

Genome size was estimated for the *Poa* reference individual and four of the population panel individuals (Supplementary Table S5). Not all population panel individuals were sampled as some plants died prior to estimation. Genome size estimation methods using an internal standard are modified from Doležel *et al.* (2007). Two internal standards were used for the reference: maize B73 inbred line (5.16 pg/2C) and *A. gerardi* accession CAM 1351 (6.13 pg/2C). Only the maize B73 internal standard was used for the population panel. Approximately 10 × 1 cm of fresh leaf tissue for the target and sample standard were placed in a plastic square petri dish. A chopping solution composed of 1 mL LB01 buffer solution, 250 μL propidium iodide (PI) stock (2 mg/mL), and 25 μL RNase (1 mg/mL) was added to the dish (1.25 mL; Doležel *et al.* 2007). The tissue was then chopped into 2–4 mm lengths and the chopping solution was mixed through the leaves by pipetting. The solution was then pipetted through a 30 μm sterile single-pack CellTrics filter into a 2 mL Rohren tube on ice. Three replicates were chopped separately and analyzed for each *Poa* population panel genotype and nine replicates were analyzed for the reference. The samples were left to chill for 20 min before analysis with a BD Accuri C6 flow cytometer. Samples were run in Auto Collect mode with a 5-min run limit, slow fluidics option, a foward scatter height (FSC-H) threshold with less than 200,000 events, and a one-cycle wash. The cell count, coefficient of variation of FL2-A, and mean FL2-A were recorded for the target and reference sample with no gating. Results were analyzed separately for each replicate and manually annotated to designate the set of events. The replicates for each *Poa* genotype were averaged (Supplementary Table S6).

Illumina sequencing of the *Poa* population panel

DNA was extracted from the *Poa* population panel using approximately 100 mg of lyophilized leaf tissue and a DNeasy Plant Kit (Qiagen Inc., Germantown, MD). High throughput Illumina Nextera libraries were constructed and samples were sequenced with other plant samples in pools of 96 individuals in one lane of an S4 flowcell in an Illumina Novaseq 6000 System with paired-end 150-bp reads, providing approximately 0.80× coverage for each sample.

Species identification

Species identification was completed using both morphological and DNA sequence data. Morphological assessment was completed for the *Poa* reference genome and three of the population panel samples using flowering and vegetative vouchers. Phylogenetic inference was completed for species identification of all samples using one plastid and two nuclear ribosomal DNA loci: *trn*T-*trn*L-*trn*F (TLF), external transcribed spacer (ETS), and internal transcribed spacer (ITS), respectively. Trees for *mat*K and *rpo*B-*trn*C were also evaluated but the sequences showed little variation across sampled species.

Sequences for these loci were extracted from the *Poa* population panel whole genome sequence data by aligning reads to a *P. pratensis* sequence for each locus downloaded from Genbank (Supplementary Table S2) using the default options of bwa mem (v0.7.17; Li 2013). The alignment files were sorted using SAMtools (v1.7; Danecek *et al.* 2021), read groups were added using Picard AddOrReplaceReadGroups, and duplicates removed with Picard MarkDuplicates using default settings (http://broadinstitute.github.io/picard). We identified variable sites for each sample separately using Genome Analysis Toolkit (GATK; v4.1) HaplotypeCaller with default options (Van der Auwera and O'Connor 2020). SNPs were filtered to remove sites with low mapping quality and low sequencing quality (`gatk VariantFiltration -filter "QUAL < 40.0" -filter "MQ < 40.0"` and default `gatk SelectVariants`). A consensus sequence for each locus and sample was generated using GATK FastaAlternateReferenceMaker, which replaces the gene reference bases at variable sites with the alternate allele.

Sequences were extracted from the reference genome by aligning the *P. pratensis* reference sequences downloaded from Genbank to the reference genome with bwa mem using default options (v0.7.17; Li 2013). This allowed us to identify the position of each locus in the reference. Each locus only mapped to a single region in the reference genome, which was extracted using bioawk (https://github.com/lh3/bioawk).

Sequences from the reference genome and the population panel were included in a dataset with 119 *Poa* samples from previous work (Supplementary Table S3; Gillespie *et al.* 2007, 2008, 2009; Refulio-Rodriguez *et al.* 2012; Soreng *et al.* 2015; Cabi *et al.* 2016; Giussani *et al.* 2016; Cabi *et al.* 2017; Soreng *et al.* 2017; Gillespie *et al.* 2018; Soreng and Gillespie 2018; Soreng *et al.* 2020; Sylvester *et al.* 2021). These samples were chosen to represent the phylogenetic diversity of the genus *Poa* and include all seven currently recognized subgenera as well as 29 of 38 sections and several unclassified species groups (classification according to Gillespie *et al.* 2007, with updates by Gillespie *et al.* 2008; Cabi *et al.* 2017; Gillespie *et al.* 2018; Soreng and Gillespie 2018; Soreng *et al.* 2020). Since formal infrageneric taxonomic delimitations are often imperfect, and the genus *Poa* is large and highly complex, genotype codes are used in Supplementary Table S3 as shorthand for the plastid and nrDNA clades found in a sample or species (see Soreng *et al.* 2020 for the most recent iterations).

Sequences were aligned using the auto-select algorithm and default parameters in the Multiple Alignment using Fast Fourier Transform (MAFFT) plugin (v7.017; Katoh and Standley 2013) in Geneious (v8.1.9; http://www.geneious.com) followed by manual adjustment. *Poa* sect. *Sylvestres* was used as the outgroup to root trees based on its strongly supported position as sister to all other *Poa* species in previous plastid analyses (Gillespie *et al.* 2007, 2009, 2018). Bayesian Markov chain Monte Carlo analyses were conducted in MrBayes (v3.2.6; Ronquist *et al.* 2012). Optimal models of molecular evolution were determined using the akaike information criterion (AIC; Akaike 1974) conducted through likelihood searches in jModeltest (Darriba *et al.* 2012) with default settings. Models were set at `GTR + Γ` for ETS and `GTR + I + Γ` for ITS and TLF based on the AIC scores and the models allowed in MrBayes. Two independent runs of four chained searches were performed for three or four million generations, sampling every 500 generations, with default parameters. Analyses were stopped when an average standard deviation of split frequencies of 0.007001, 0.006350, and 0.006490 was reached for ITS, ETS, and TLF, respectively. A 25% burn-in was implemented prior to

summarizing a 50% majority rule consensus tree and calculating Bayesian posterior probabilities. Trees were visualized and annotated in R using ggtree (v2.0.4) with ape (v5.4) and treeio (v1.10) (R Core Team 2017; Paradis and Schliep 2019; Wang *et al.* 2020; Yu 2020).

Genome assembly

PacBio subreads obtained as binary sequency alignment/map (BAM) files were converted to FASTA format using SAMtools (v1.10; Danecek *et al.* 2021) and error correction was performed using overlap detection and error correction module (first stage) of Falcon (v1.8.0; Chin *et al.* 2016). For running Falcon, the following options were used: the expected genome size was set to 6.4 Gbp (`-genome_size = 6400000000`), a minimum of two reads, maximum of 200 reads, and minimum identity of 70% for error corrections (`--min_cov 2 --max_n_read 200, --min_idt 0.70`), using the 40× seed coverage for auto-calculated cutoff. The average read correction rate was set to 75% (`-e 0.75`) with local alignments at a minimum of 3,000 bp (`-l 3000`) as suggested by the Falcon manual. For the DAligner step, the exact matching length of k-mers between two reads was set to 18 bp (`-k 18`) with a read correction rate of 80% (`-e 0.80`) and local alignments of at least 1,000 bp (`-l 1000`). Genome assembly was performed with Canu (v1.9: Koren *et al.* 2017) using the error-corrected reads from Falcon. For sequence assembly, the corrected reads had over 70× coverage for the expected genome size of *Poa* and were characterized by N50 of 25.6 kbp and average length of 16.3 kbp. These reads were trimmed and assembled with Canu using the default options except for `ovlMerThreshold=500`.

The Canu generated contig assembly was further scaffolded utilizing the Bionano optical map with Bionano Solve (v3.4) and Bionano Access (v1.3.0), as described previously by Hufford *et al.* (2021). The default config file (hybridScaffold_DLE1_config.xml) and the default parameters file (optArguments_nonhaplotype_noES_noCut_DLE1_saphyr.xml) were used for the hybrid assembly. The scaffolding step of Bionano Solve incorporates three types of gaps: (1) gaps of estimated size (varying N-size, but not 100 bp or 13 bp), using calibrated distance conversion of optical map to basepair (cases when contiguous optical map connects two contigs); (2) gaps of unknown sizes (100-N gaps), when distance could not be estimated (cases when large repeat regions like rDNA or centromeres interrupt the optical map but evidence to connect the map is present); and (3) 13-N gaps, in regions where two or more independently assembled contigs align to the same optical map, overlapping at the ends. The 13-N gaps are usually caused by sequence similarity sufficient for aligning to the optical map, but less than required to merge contigs. This could be caused by either high heterozygosity in that region, highly repetitive sequence, paralogous regions of the subgenomes, or assembly errors. The contig overlaps, regardless of the size, are connected end-to-end by adding 13-N gaps when processed using Bionano Solve. Due to the polyploid nature of Poa as well as its high heterozygosity, these 13-N gaps had to be manually curated. We inspected the contig alignments to the optical map using Bionano Access (v1.3.0), either to trim the overlapping sequence or to remove exact duplicates to generate error-free assembly.

Genome annotation

Gene prediction was carried out using a comprehensive method combining ab initio predictions (from BRAKER v2.1.6; Brna *et al.* 2021) with direct evidence (inferred from transcript assemblies) using the BRAKER-Inferred Directly (BIND) strategy (Li *et al.* 2021). Briefly, 58 RNA-seq libraries were downloaded from NCBI (Supplementary Table S4) and mapped to the genome using a STAR (v2.5.3a; Dobin *et al.* 2013)-indexed genome and an iterative two-pass approach under default options to generate mapped BAM files. BAM files were used as input for multiple transcript assembly programs to assemble transcripts: Class2 (v2.1.7; Song *et al.* 2016), Cufflinks (v2.2.1; Trapnell *et al.* 2012), Stringtie (v2.1.4; Pertea *et al.* 2015), and Strawberry (v1.1.2; Liu and Dickerson 2017). Redundant assemblies were collapsed and the best transcript for each locus was picked using Mikado (v2.3.3; Venturini *et al.* 2018) by filling in the missing portions of the ORF using TransDecoder (v5.5.0; Haas *et al.* 2013) and homology as informed by the NCBI Basic Local Alignment Seach Tool (BLASTx) (v2.10.1+; Altschul *et al.* 1990) results to the SwissProtDB (Duvaud *et al.* 2021). Splice junctions were also refined using Portcullis (v1.2.1; Mapleson *et al.* 2018) to identify isoforms and to correct misassembled transcripts. Both ab initio and direct evidence predictions were analyzed with TESorter (v1.3.0; Zhang *et al.* 2019) to identify and remove any TE-containing genes before merging them. Merging was done using the GeMoMa (v1.8) Annotation Filter tool to combine and filter gene predictions from BRAKER, Mikado and additional homology-based gene predictions generated by the GeMoMa pipeline using *Hordeum vulgare* annotations (Keilwagen *et al.* 2016, 2018; Mascher *et al.* 2021). The predictions were prioritized using weights, with highest for homology (1.0), followed by direct evidence (0.9) and lowest for gene predictions from ab initio methods (0.1). Homology is defined by GeMoMa as protein sequence similarity and intron position conservation relative to *Hordeum vulgare*. The Annotation Filter tool was run with settings to enforce the completeness of the prediction (`start=='M' stop=='*'`), external evidence support (`score/aa>=0.75`), and RNAseq support (`evidence>1` or `tpc==1.0`). The final predictions were subjected to phylostratiography analyses using phylostratr (v0.20; Arendsee *et al.* 2019). The focal species were set as "4545" for *P. pratensis*, and default options were used. The program creates a clade tree of species based on the current NCBI tree of life, trims the tree to maximize evolutionary diversity, retrieves the species proteome from Uniprot, and compares the proteins of the focal species to those of other species in the tree using pairwise BLASTs (Diamond search). Each gene is then assigned to the deepest clade in which it has an inferred homolog. Genes found only in the focal species are considered orphan genes and assigned to the phylostratum "*P. pratensis*." Final gene-level annotations were saved in GFF3 format and the predicted peptides/coding sequence sequences were extracted using `gffread` of the Cufflinks package (v2.2.1; Trapnell *et al.* 2012).

Assessment of the assembly

Genome contiguity statistics were computed using the Assemblathon script (Bradnam *et al.* 2013). Gene space completeness was measured using Benchmarking Universal Single-Copy Orthologs (BUSCO, v4.0; Manni *et al.* 2021) using the liliopsida_odb10 profile ($n = 3,278$) and poales_odb10 profile ($n = 4,896$) with default options. The contiguity of TE assembly was then assessed using the LTR Assembly Index (LAI; Ou *et al.* 2018). To compute LAI, we first annotated repeats using the Extensive de novo TE Annotator (EDTA; v1.9.6; Ou *et al.* 2019), and intact LTR retrotransposons (LTR-RTs) were identified using LTRharvest (v1.6.1; Manchanda *et al.* 2020) and LTR_FINDER_parallel (v1.1; Ellinghaus *et al.* 2008). LTR_retriever (v2.9.0; Ou *et al.* 2018) was then used to filter the intact LTRs and computed the LAI score for the genome.

Population genetics of *Poa*

The population panel was mapped to the scaffold assembly, excluding the alternate scaffolds, using bwa mem (v0.7.17; Li 2013). Reads

were sorted using SAMtools (v1.7; Danecek et al. 2021), read groups were added using Picard AddOrReplaceReadGroups, and duplicates removed with Picard MarkDuplicates (http://broadinstitute.github.io/picard) using default settings.

Site filtering and genotyping were completed with ANGSD (v0.934; Korneliussen et al. 2014). Reads were filtered, retaining unique reads, reads with a flag below 255, and proper pairs (`angsd -uniqueOnly 1 -remove_bads 1 -only_proper_pairs 1 -trim 0`), as well as a minimum mapping and base quality of 30 (`angsd -minMapQ 30 -minQ 30`). Sites were filtered with a strict maximum depth cutoff in order to exclude sites where paralogs may be mapping. Assuming read depth follows a Poisson distribution with a mean of 0.8, and we expect 99% of reads to have a depth of 4 or less. We included sites with a minimum depth of 1 and a maximum depth of 4 and required all genotypes to have data at a site (`angsd -doCounts 1 -setMinDepthInd 1 -setMaxDepthInd 4 -minInd 8`). Sites were also filtered for a minor allele frequency greater than 5% in the principal component analysis (PCA; `angsd -doMajorMinor 4 -doCounts 1 -doMaf 1 -minMaf 0.05`).

After filtering, a single-read was randomly sampled at each base to serve as the genotype (`angsd -doIBS 1`). This genotyping approach is discussed in Results and Discussion. A genotype matrix was sampled three independent times for each of the following analyses in order to assess sampling error.

Population structure and nucleotide diversity were evaluated to demonstrate the utility of the *P. pratensis* reference genome. Population structure was assessed using a PCA implemented in ANGSD (`angsd -doCov`). A PCA was run with all *Poa* and only *P. pratensis*. The covariance matrices were plotted with ggplot2 (v3.4) in R (Wickham 2016; R Core Team 2017).

Nucleotide diversity was estimated for each *P. pratensis* genotype in the *Poa* population panel as nucleotide diversity per genome using a custom R script. We are defining nucleotide diversity per genome as the number of sites with the reference allele divided by the total number of sites. Only sites that met our filtering criteria and contained no missing data across *P. pratensis* genotypes were included. Results were plotted with ggplot2 in R.

Results and discussion

Species identification and validation

Herbarium vouchers for the *Poa* reference genome and two of the population panel genotypes were identified as *P. pratensis* by their morphology (Supplementary Table S1). The *Poa* reference genotype can be further classified as subspecies *angustifolia*, characterized by narrower and involute leaf blades, usually with strigose hairs on the adaxial surface of blades. The blades of *P. pratensis* subspecies *angustifolia* are firmer and tend to be more consistently glaucous. The intravaginal shoots are often disposed in fascicles of more than one shoot, the inflorescences are generally narrower, and the spikelets are smaller than other *P. pratensis* subspecies (Soreng and Barrie 1999; Soreng 2007; Cope and Gray 2009). *P. pratensis* subspecies *angustifolia* is the most likely classification for the reference genotype, although the infraspecies structure is complex and the subspecies genetically and morphologically grade into one another (Soreng and Barrie 1999; Soreng 2007; Cope and Gray 2009).

The remaining *Poa* population genotypes did not survive long enough for detailed morphological identification. We identified the remaining genotypes and confirmed the morphological IDs, using phylogenetic inference with three commonly used loci (ETS, ITS, and TLF). The reference genome was identified as *P. pratensis* by all three loci (Supplementary Figures S1–S3). Seven of the eight genotypes in the *Poa* population panel were identified as *P. pratensis* by two of the three loci (ITS and ETS; Supplementary Figures S1 and S2 and Table S1) and held an unresolved position within the subgenus *Poa* in the third tree (TLF; Supplementary Figure S3). The eighth population panel genotype was identified as *P. compressa* L. by all three loci. Phylogenetic identification thus supports our morphological identification of the reference genome as *P. pratensis*.

Genome size and ploidy estimation

The reference individual was estimated to be octoploid given a genome size estimate of 3,525 Mbp and chromosome count of 54, assuming a basic chromosome number of $x = 7$ and a loss of two chromosomes (Supplementary Figure S4 and Table S5; Avdulov 1931; Grass Phylogeny Working Group et al. 2001). Further cytological studies are required to understand whether the chromosome loss is due to deletion or rearrangement. Our genome size estimate falls within the large range of genome sizes reported for *P. pratensis*, 2–9 pg/1C (Huff and Bara 1993; Barcaccia et al. 1997; Eaton et al. 2004; Raggi et al. 2015).

We also estimated the genome size of four of the eight population panel individuals. Genome size ranged from 3,248 to 4,856 Mbp with genotypes from the same population having similar genome sizes (Supplementary Table S5). The substantial range in genome size variation in the population panel is not unexpected as *P. pratensis* is a polyploid series with common aneuploidy (Huff 2010). Given the range in the population panel, it is likely the genotypes have different chromosome counts and ploidy.

Genome assembly

Error-corrected PacBio reads (100 Gb; 70× coverage) were assembled into 27,953 contigs. The contig assembly was oriented and further scaffolded using a Bionano optical map resulting in 118 primary scaffolds and 10 alternate scaffolds (Table 1).

The assembly is approximately 173% of the genome size (Table 1). Completeness of the assembly was assessed using BUSCO and the LAI. The assembly contains 99% of the expected conserved genes (BUSCOs), 98% of which were duplicated, and a LAI value of 25.8 indicates the transposable element assembly is also complete (Ou et al. 2018). Given the assembled genome size is approximately two-times the size of the estimated genome size and nearly all detected BUSCOs are duplicated, two unphased haplotypes are likely present in the assembly. Additionally, the high rate of duplicated BUSCOs may also be due to similarity among *Poa* subgenomes.

Table 1. Assembly statistics.

Variable	Description
Scaffolds	118
Contigs	8,391
Estimated genome size	3.521 Gbp
Assembled genome size	6.09 Gbp
Scaffold N50	65,127,037 bp
Scaffold L50	31
Contig N50	1,095,498 bp
Contig L50	1,548
Longest scaffold	177,118,352 bp
Scaffolds >1 Mb	110
Scaffolds >10 Mb	98
Average scaffold length	51,622,171 bp
Average length of gaps	44,233 bp
Complete BUSCOs	99.2%
LAI	25.8

Genome annotation

We identified 256,281 gene models, approximately 32K per subgenome assuming octoploidy, using a hybrid gene prediction pipeline that combined ab initio gene models with direct evidence annotations. Phylostrata demonstrated approximately 13% of the gene models are species-specific, which is higher than would be expected from orphan genes alone (Arendsee *et al.* 2014). Since the phylostratr program uses full proteomes from Uniprot to classify genes to their phylostrata, and there is lack of high-quality representative genomes for this clade, we observed an excess of species-specific genes. This demonstrates the important gap a *P. pratensis* reference genome fills in the green tree of life.

Transposable elements were comprehensively annotated using EDTA (Ou *et al.* 2019) and found to compose 58% of the genome. More specifically, Class I LTR-RTs and Class II DNA transposons comprise 36% and 15% of the genome, respectively. At the level of superfamily, the RLG (*Ty3*) LTR-RT superfamily was the most common at 18% of the genome.

Application of the reference genome

The reference genome contains multiple unphased haplotypes, and care should be taken in analyses that require genotypes or allele frequencies. Briefly, we discuss an alternative framework for estimating allele frequencies and potential pitfalls. Diploid genotypes (AA, Aa, and aa) should not be called, as at least two haplotypes are assembled for many reference positions. Instead, we utilized an approach in which we randomly sampled a read from each position (Green *et al.* 2010). The randomly sampled read can then be used to calculate population allele frequencies and pairwise genetic distance matrices that are unbiased to sequencing depth or ploidy (Green *et al.* 2010; Pečnerová *et al.* 2021; van der Valk *et al.* 2021). Although we do not detect a bias due to ploidy or chromosome count in our analyses (see below), these factors should always be considered in interpretation of results.

Population genetics of North American Poa

Here, we demonstrate the effectiveness of the reference genome and a single-read genotyping approach in the estimation of population structure, using PCA and nucleotide diversity.

A PCA was run separately for all *Poa* genotypes, using 74,876 sites, and only *P. pratensis* genotypes, using 140,458 sites. The single-read genotypes were generated three times for the same set of sites and demonstrated similar results. We present the results for one run here. In the PCA with all *Poa* samples, most genetic variation was explained by species (27.9%) followed by population (16.2%; Fig. 1a). *P. compressa* is distantly related to *P. pratensis* (Supplementary Figures S1–S3), therefore we would expect the first principal component (PC) to separate by species. The second PC separates the *P. pratensis* genotypes in the Colorado population from two Manitoba *P. pratensis* genotypes (Fig. 1a), while genotypes from the Colorado population remain clustered. The third PC further separates the three *P. pratensis* populations.

The *P. pratensis*-only PCA demonstrates similar results with the first PC (24.6%) separating the Colorado genotypes from the two genotypes from Manitoba (Supplementary Figure S5). The second PC (15.8%) separates the two genotypes from Manitoba and separates one Colorado genotype from the cluster. These results suggest that North American *P. pratensis* populations are genetically differentiated and exhibit population structure, rather than being highly homogeneous or clonal. Our results support previous findings of population divergence in Northern Great Plains populations (Dennhardt *et al.* 2016).

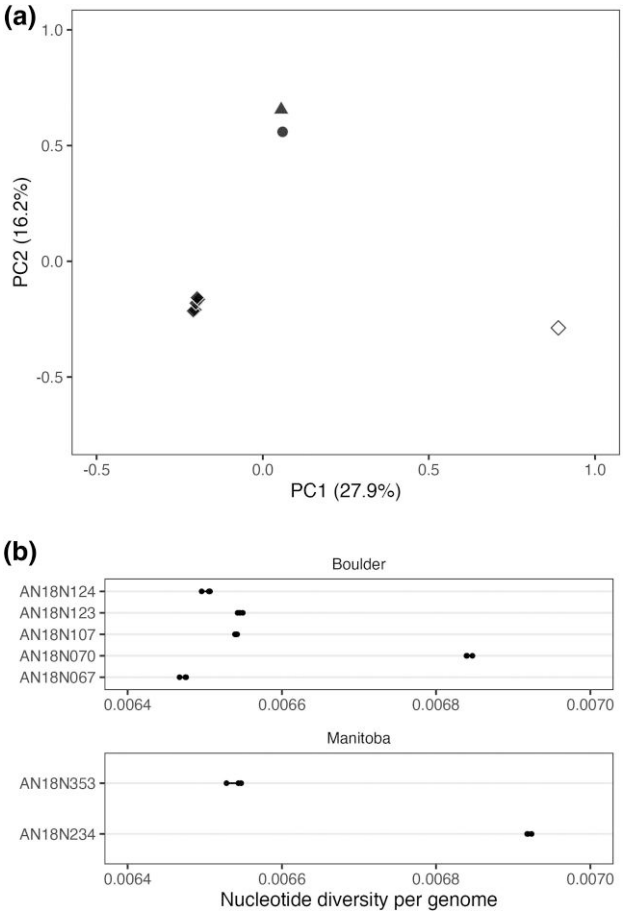

Fig. 1. Population structure of *Poa* and nucleotide diversity in *P. pratensis*. (a) The first two PCs of a PCA of all sequenced *Poa* genotypes. The percent of genetic variation explained by each PC is reported in parentheses on each axis. Sample locations are indicated by shape (circle = Argyle, Manitoba; triangle = Tolstoi, Manitoba; diamond = Boulder, Colorado) and species are colors (white = *P. compressa*; black = *P. pratensis*). (b) Mean nucleotide diversity per genome for only *P. pratensis* genotypes. Mean diversity of each run is plotted as a black circle for all genotypes.

To further understand the structure of genetic diversity across *P. pratensis* populations and the clustering within the Colorado population, we estimated nucleotide diversity per genome using 20,149,358 sites. Single-read genotypes were randomly drawn and nucleotide diversity was calculated three times with little variation between runs (Fig. 1b; average variation between runs = 2.85×10^{-11}). Mean diversity across *P. pratensis* genotypes is high ($\pi =$ 0.0066, SD = 0.00017), which is consistent with previous studies of *P. pratensis* (Honig *et al.* 2012; Bonos and Huff 2013; Bushman *et al.* 2013; Raggi *et al.* 2015; Honig *et al.* 2018). The range of mean nucleotide diversity per genome within the Colorado population (0.0065–0.0068) and between the Manitoba genotypes (0.065–0.0069) is large, suggesting high within-population diversity.

Conclusions

P. pratensis is a globally popular turfgrass species used in lawns and recreation areas. Despite its economic value, progression of molecular tools to aid breeding has been slow compared to other turfgrasses as a result of polyploidy and apomixis (Bushman and Warnke 2013). Utilizing long read technology and a Bionano optical map, we have assembled and annotated the first high-quality *P. pratensis* reference genome. We demonstrated the utility and

application of the reference genome by evaluating the genetic diversity and population structure of wild North American *Poa*. As a result, we provided the first estimate of nucleotide diversity in *P. pratensis*.

Since our initial manuscript submission and preprint, Robbins *et al.* (2023) have published the genome of *P. annua*, a distantly related *Poa* species known as a weed and turfgrass world-wide. Future analyses, beyond the scope of this paper, comparing the two genomes will likely be fruitful for understanding the global success of *P. pratensis* and *P. annua*. As such, the *P. pratensis* reference genome and annotation will serve as an important resource in the study of bluegrasses.

Data availability

The genome assembly and annotation are available from the European Nucleotide Archive under BioProject PRJEB51672. The raw Illumina sequence data for the *Poa* population panel is available from NCBI Sequence Read Archive under BioProject ID PRJNA730042. The code for the entirety of assembly, annotation, and population genetic analyses is documented at https://github.com/phillipsar2/poa˙genome. Supplementary material is available at G3 online.

Acknowledgments

Thank you to Dr. Chrissy McAllister and Bess Bookout for sharing samples collected with permission from Nature Conservancy Canada properties and Lynn Riedel for collection of samples with permission from the City of Boulder Open Space and Mountain Parks. The Texas Advanced Computing Center (TACC) at The University of Texas at Austin and HPC@ISU equipment at Iowa State University (partially funded by NSF under MRI grant number 1726447) provided HPC resources that have contributed to the research results reported within this paper. We thank Dr. Kevin Fengler (for providing assembly instructions) and Dr. Gina Zastrow-Hayes (for establishing sequencing contracts) of Corteva Agriscience for their help in this project. ARP would like to thank Andrew L. Murray for his support throughout the duration of this project. Additionally, the authors would like to thank our *A. gerardi* reference plant for being contaminated with *Poa* and Felix Andrews for his alleged role in the happy accident that led to this work. Finally, thank you to Bob Ross for inspiring a generation of scientists to persevere.

Funding

This project was funded by the National Science Foundation (NSF) grant number 1822330. HPC resources at TACC were partially funded by NSF under MRI grant number 1726447.

Conflicts of interest

The authors declare no conflict of interest.

Literature cited

Akaike H. A new look at the statistical model identification. IEEE Trans Autom Control. 1974;19:716–723.

Albertini E, Marconi G, Barcaccia G, Raggi L, Falcinelli M. Isolation of candidate genes for apomixis in *Poa pratensis* L. Plant Mol Biol. 2004;56:879–894.

Altschul SF, Gish W, Miller W, Myers EW, Lipman DJ. Basic local alignment search tool. J Mol Biol. 1990;215:403–410.

Arendsee Z, Li J, Singh U, Seetharam A, Dorman K, Wurtele ES, Schwartz R. phylostratr: a framework for phylostratigraphy. Bioinformatics. 2019;35:3617–3627.

Arendsee ZW, Li L, Wurtele ES. Coming of age: orphan genes in plants. Trends Plant Sci. 2014;19:698–708.

Avdulov N. Kario-sistematicheskoye issledovaniye semeystva zlakov (Karyosystematic studies in the grass family). Bull Appl Bot Gen Pl Breed Leningrad. 1931;44:1–428.

Barcaccia G, Mazzucato A, Belardinelli A, Pezzotti M, Lucretti S, Falcinelli M. Inheritance of parental genomes in progenies of *Poa pratensis* L. from sexual and apomictic genotypes as assessed by RAPD markers and flow cytometry. Theor Appl Genet. 1997;95:516–524.

Grass Phylogeny Working Group, Barker NP, Clark LG, Davis JI, Duvall MR, Guala GF, Hsiao C, Kellogg EA, Linder HP, Mason-Gamer R, *et al.* Phylogeny and subfamilial classification of the grasses (Poaceae). Ann MO Bot Gard. 2001;88:373–457.

Bonos SA, Huff DR. Cool-season grasses: biology and breeding. Turfgrass. 2013;56:591–660.

Bradnam KR, Fass JN, Alexandrov A, Baranay P, Bechner M, Birol I, Boisvert S, Chapman JA, Chapuis G, Chikhi R, *et al.* Assemblathon 2: evaluating de novo methods of genome assembly in three vertebrate species. GigaScience. 2013;2:2047–217X.

Brnăa T, Hoff KJ, Lomsadze A, Stanke M, Borodovsky M. BRAKER2: automatic eukaryotic genome annotation with GeneMark-EP+ and AUGUSTUS supported by a protein database. NAR Genomics Bioinf. 2021;3:lqaa108.

Brown WL. Chromosome complements of five species of *Poa* with an analysis of variation in *Poa pratensis*. Am J Bot. 1939;26:717–723.

Bushman BS, Warnke SE. Genetic and genomic approaches for improving turfgrass. Turfgrass. 2013;56:683–711.

Bushman BS, Warnke SE, Amundsen KL, Combs KM, Johnson PG. Molecular markers highlight variation within and among Kentucky bluegrass varieties and accessions. Crop Sci. 2013;53:2245–2254.

Cabi E, Soreng RJ, Gillespie L. Taxonomy of *Poa jubata* and a new section of the genus (Poaceae). Turk J Bot. 2017;41:404–415.

Cabi E, Soreng RJ, Gillespie L, Amiri N. *Poa densa* (Poaceae), an overlooked Turkish steppe grass, and the evolution of bulbs in *Poa*. Willdenowia. 2016;46:201–211.

Carrier L, Bort KS. The history of Kentucky bluegrass and white clover in the United States. Agron J. 1916;8:256–267.

Casler MD, Duncan RR. Turfgrass Biology, Genetics, and Breeding. Hoboken: John Wiley & Sons; 2003.

Chin C-S, Peluso P, Sedlazeck FJ, Nattestad M, Concepcion GT, Clum A, Dunn C, O'Malley R, Figueroa-Balderas R, Morales-Cruz A, *et al.* Phased diploid genome assembly with single-molecule real-time sequencing. Nat Methods. 2016;13:1050–1054.

Cope TA, Gray AJ. Grasses of the British Isles. London: Botanical Society of the British Isles; 2009.

Danecek P, Bonfield JK, Liddle J, Marshall J, Ohan V, Pollard MO, Whitwham A, Keane T, McCarthy SA, Davies RM, *et al.* Twelve years of SAMtools and BCFtools. GigaScience. 2021;10:giab008.

Darriba D, Taboada GL, Doallo R, Posada D. jmodeltest 2: more models, new heuristics and parallel computing. Nat Methods. 2012;9:772–772.

DeKeyser ES, Dennhardt LA, Hendrickson J. Kentucky bluegrass (*Poa pratensis*) invasion in the Northern Great Plains: a story of rapid dominance in an endangered ecosystem. Invasive Plant Sci Manage. 2015;8:255–261.

Dennhardt LA, DeKeyser ES, Tennefos SA, Travers SE. There is no evidence of geographical patterning among invasive Kentucky bluegrass (*Poa pratensis*) populations in the Northern Great Plains. Weed Sci. 2016;64:409–420.

Dobin A, Davis CA, Schlesinger F, Drenkow J, Zaleski C, Jha S, Batut P, Chaisson M, Gingeras TR. Star: ultrafast universal RNA-seq aligner. Bioinformatics. 2013;29:15–21.

Doležel J, Greilhuber J, Suda J. Estimation of nuclear DNA content in plants using flow cytometry. Nat Protocols. 2007;2: 2233–2244.

Duvaud S, Gabella C, Lisacek F, Stockinger H, Ioannidis V, Durinx C. Expasy, the Swiss bioinformatics resource portal, as designed by its users. Nucleic Acids Res. 2021;49:W216–W227.

Eaton T, Curley J, Williamson R, Jung G. Determination of the level of variation in polyploidy among Kentucky bluegrass cultivars by means of flow cytometry. Crop Sci. 2004;44:2168–2174.

Ellinghaus D, Kurtz S, Willhoeft U. LTRharvest, an efficient and flexible software for de novo detection of LTR retrotransposons. BMC Bioinf. 2008;9:1–14.

Funk CR and Sang JH. Recurrent Intraspecific Hybridization—A Proposed Method of Breeding Kentucky Bluegrass. New Jersey Agricultural Experiment Station Bulletin, Rutgers University; 1967.

Gillespie LJ, Archambault A, Soreng RJ. Phylogeny of *Poa* (Poaceae) based on trnT–trnF sequence data: major clades and basal relationships. Aliso. 2007;23:420–434.

Gillespie LJ, Soreng RJ, Bull RD, Jacobs SW, Refulio-Rodriguez NF. Phylogenetic relationships in subtribe Poinae (Poaceae, Poeae) based on nuclear ITS and plastid trnT-trnL-trnF sequences. Botany. 2008;86:938–967.

Gillespie LJ, Soreng RJ, Cabi E, Amiri N. Phylogeny and taxonomic synopsis of *Poa* subgenus *Pseudopoa* (including *Eremopoa* and *Lindbergella*) (Poaceae, Poeae, Poinae). PhytoKeys. 2018;111: 69–102.

Gillespie LJ, Soreng RJ, Jacobs SW. Phylogenetic relationships of Australian *Poa* (Poaceae: Poinae), including molecular evidence for two new genera, *Saxipoa* and *Sylvipoa*. Aust Syst Bot. 2009;22: 413–436.

Giussani LM, Gillespie LJ, Scataglini MA, Negritto MA, Anton AM, Soreng RJ. Breeding system diversification and evolution in American *Poa* supersect. *Homalopoa* (Poaceae: Poeae: Poinae). Ann Bot. 2016;118:281–303.

Green RE, Krause J, Briggs AW, Maricic T, Stenzel U, Kircher M, Patterson N, Li H, Zhai W, Fritz MH-Y, *et al.* A draft sequence of the Neandertal genome. Science. 2010;328:710–722.

Haas BJ, Papanicolaou A, Yassour M, Grabherr M, Blood PD, Bowden J, Couger MB, Eccles D, Li B, Lieber M, *et al.* De novo transcript sequence reconstruction from RNA-seq using the trinity platform for reference generation and analysis. Nat Protocols. 2013;8: 1494–1512.

Haydu JJ, Hodges AW, Hall CR. Economic impacts of the turfgrass and lawncare industry in the United States. EDIS. 2006;2006(7): 8–11.

Heide O. Control of flowering and reproduction in temperate grasses. New Phytol. 1994;128:347–362.

Hendrickson JR, Liebig MA, Printz J, Toledo D, Halvorson JJ, Christensen RG, Kronberg SL. Kentucky bluegrass impacts diversity and carbon and nitrogen dynamics in a Northern Great Plains rangeland. Rangeland Ecol Manage. 2021;79:36–42.

Honig JA, Averello V, Bonos SA, Meyer WA. Classification of Kentucky bluegrass (*Poa pratensis* L.) cultivars and accessions based on microsatellite (simple sequence repeat) markers. HortScience. 2012;47:1356–1366.

Honig JA, Averello V, Kubik C, Vaiciunas J, Bushman BS, Bonos SA, Meyer WA. An update on the classification of Kentucky bluegrass cultivars and accessions based on microsatellite (SSR) markers. Crop Sci. 2018;58:1776–1787.

Huff DR. Chapter 15: Bluegrasses. In: Handbook of Plant Breeding: Fodder Crops and Amenity Grasses. Manhattan: Springer; 2010. p. 345–379.

Huff DR, Bara JM. Determining genetic origins of aberrant progeny from facultative apomictic Kentucky bluegrass using a combination of flow cytometry and silver-stained RAPD markers. Theor Appl Genet. 1993;87:201–208.

Hufford MB, Seetharam AS, Woodhouse MR, Chougule KM, Ou S, Liu J, Ricci WA, Guo T, Olson A, Qiu Y, *et al.* De novo assembly, annotation, and comparative analysis of 26 diverse maize genomes. Science. 2021;373(6555):655–662.

Kato A. Air drying method using nitrous oxide for chromosome counting in maize. Biotech Histochem. 1999;74:160–166.

Kato A, Lamb JC, Albert PS, Danilova T, Han F, Gao Z, Findley S, Birchler JA. Chromosome painting for plant biotechnology. In: Plant Chromosome Engineering. Springer, Manhattan; 2011. p. 67–96.

Kato A, Lamb JC, Birchler JA. Chromosome painting using repetitive DNA sequences as probes for somatic chromosome identification in maize. Proc Natl Acad Sci USA. 2004;101:13554–13559.

Katoh K, Standley DM. MAFFT multiple sequence alignment software version 7: improvements in performance and usability. Mol Biol Evol. 2013;30:772–780.

Keilwagen J, Hartung F, Paulini M, Twardziok SO, Grau J. Combining RNA-seq data and homology-based gene prediction for plants, animals and fungi. BMC Bioinf. 2018;19:1–12.

Keilwagen J, Wenk M, Erickson JL, Schattat MH, Grau J, Hartung F. Using intron position conservation for homology-based gene prediction. Nucleic Acids Res. 2016;44:e89–e89.

Koren S, Walenz BP, Berlin K, Miller JR, Bergman NH, Phillippy AM. Canu: scalable and accurate long-read assembly via adaptive k-mer weighting and repeat separation. Genome Res. 2017;27: 722–736.

Korneliussen TS, Albrechtsen A, Nielsen R. ANGSD: analysis of next generation sequencing data. BMC Bioinf. 2014;15:356.

Kral-O'Brien KC, Limb RF, Hovick TJ, Harmon JP. Compositional shifts in forb and butterfly communities associated with Kentucky bluegrass invasions. Rangeland Ecol Manage. 2019;72: 301–309.

Li H. Aligning sequence reads, clone sequences and assembly contigs with BWA-MEM. arXiv:1303.3997; 2013.

Li J, Singh U, Bhandary P, Campbell J, Arendsee Z, Seetharam AS, Wurtele ES. Foster thy young: enhanced prediction of orphan genes in assembled genomes. Nucleic Acids Res. 2021;50: gkab1238.

Liu R, Dickerson J. Strawberry: fast and accurate genome-guided transcript reconstruction and quantification from RNA-seq. PLoS Comput Biol. 2017;13:e1005851.

Manchanda N, Portwood JL, Woodhouse MR, Seetharam AS, Lawrence-Dill CJ, Andorf CM, Hufford MB. GenomeQC: a quality assessment tool for genome assemblies and gene structure annotations. BMC Genomics. 2020;21:1–9.

Manni M, Berkeley MR, Seppey M, Simao FA, Zdobnov EM. BUSCO update: novel and streamlined workflows along with broader and deeper phylogenetic coverage for scoring of eukaryotic, prokaryotic, and viral genomes. arXiv:2106.11799; 2021.

Mapleson D, Venturini L, Kaithakottil G, Swarbreck D. Efficient and accurate detection of splice junctions from RNA-seq with portcullis. GigaScience. 2018;7:giy131.

Marconi G, Aiello D, Kindiger B, Storchi L, Marrone A, Reale L, Terzaroli N, Albertini E. The role of apostart in switching between sexuality and apomixis in *Poa pratensis*. Genes. 2020;11:941.

Mascher M, Wicker T, Jenkins J, Plott C, Lux T, Koh CS, Ens J, Gundlach H, Boston LB, Tulpová Z, *et al.* Long-read sequence assembly: a technical evaluation in barley. Plant Cell. 2021;33:1888–1906.

Matzk F. New efforts to overcome apomixis in *Poa pratensis* L. Euphytica. 1991;55:65–72.

Milesi C, Running SW, Elvidge CD, Dietz JB, Tuttle BT, Nemani RR. Mapping and modeling the biogeochemical cycling of turf grasses in the United States. Environ Manage. 2005;36:426–438.

Ou S, Chen J, Jiang N. Assessing genome assembly quality using the LTR assembly index (LAI). Nucleic Acids Res. 2018;46: e126–e126.

Ou S, Su W, Liao Y, Chougule K, Agda JRA, Hellinga AJ, Lugo CSB, Elliott TA, Ware D, Peterson T, *et al.* Benchmarking transposable element annotation methods for creation of a streamlined, comprehensive pipeline. Genome Biol. 2019;20:1–18.

Paradis E, Schliep K. ape. Bioinformatics. 2019;35:526–528.

Pečnerová P, Garcia-Erill G, Liu X, Nursyifa C, Waples RK, Santander CG, Quinn L, Frandsen P, Meisner J, Stæger FF, *et al.* High genetic diversity and low differentiation reflect the ecological versatility of the African leopard. Curr Biol. 2021;31:1862–1871.

Pepin GW, Funk CR. Intraspecific hybridization as a method of breeding Kentucky bluegrass (*Poa pratenis* L.) for turf. Crop Sci. 1971;11: 445–448.

Pertea M, Pertea GM, Antonescu CM, Chang T-C, Mendell JT, Salzberg SL. StringTie enables improved reconstruction of a transcriptome from RNA-seq reads. Nat Biotechnol. 2015;33:290–295.

Raggi L, Bitocchi E, Russi L, Marconi G, Sharbel TF, Veronesi F, Albertini E, Prasad M. Understanding genetic diversity and population structure of a *Poa pratensis* worldwide collection through morphological, nuclear and chloroplast diversity analysis. PLoS ONE. 2015;10:e0124709.

R Core Team. *R: a language and environment for statistical computing*. Vienna, Austria: R Foundation for Statistical Computing; 2017.

Refulio-Rodriguez NF, Columbus JT, Gillespie LJ, Peterson PM, Soreng RJ. Molecular phylogeny of *Dissanthelium* (Poaceae: Pooideae) and its taxonomic implications. Syst Bot. 2012;37:122–133.

Robbins MD, Bushman BS, Huff DR, Benson CW, Warnke SE, Maughan CA, Jellen EN, Johnson PG, Maughan PJ, Tenaillon M. Chromosome-scale genome assembly and annotation of allotetraploid annual bluegrass (*Poa annua* L.). Genome Biol Evol. 2023;15:evac180.

Ronquist F, Teslenko M, van der Mark P, Ayres DL, Darling A, Höhna S, Larget B, Liu L, Suchard MA, Huelsenbeck JP. MrBayes 3.2: efficient Bayesian phylogenetic inference and model choice across a large model space. Syst Biol. 2012;61:539–542.

Song L, Sabunciyan S, Florea L. CLASS2: accurate and efficient splice variant annotation from RNA-seq reads. Nucleic Acids Res. 2016; 44:e98–e98.

Soreng RJ. *Poa* L. In: Flora of North America, Poaceae, Part 1, Vol. 24. Oxford University Press, Oxford; 2007.

Soreng RJ, Barrie FR. (1391) Proposal to conserve the name *Poa pratensis* (Gramineae) with a conserved type. Taxon. 1999;48:157–159.

Soreng RJ, Gillespie LJ. *Poa secunda* J. Presl (Poaceae): a modern summary of infraspecific taxonomy, chromosome numbers, related species and infrageneric placement based on DNA. PhytoKeys. 2018;(110):101–121.

Soreng R, Gillespie L, Consaul L. Taxonomy of the *Poa laxa* group, including two new taxa from Arctic Canada and Greenland, and Oregon, and a re-examination of *P.* sect. *Oreinos* (Poaceae). Nord J Bot. 2017;35:513–538.

Soreng RJ, Gillespie LJ, Koba H, Boudko E, Bull RD. Molecular and morphological evidence for a new grass genus, *Dupontiopsis* (Poaceae tribe Poeae subtribe Poinae s.l.), endemic to alpine Japan, and implications for the reticulate origin of *Dupontia* and *Arctophila* within Poinae s.l. J Syst Evol. 2015; 53:138–162.

Soreng RJ, Olonova MV, Probatova NS, Gillespie LJ. Breeding systems and phylogeny in *Poa*, with special attention to Northeast Asia: the problem of *Poa shumushuensis* and sect. *Nivicolae* (Poaceae). J Syst Evol. 2020;58:1031–1058.

Sylvester SP, Soreng RJ, Gilliespie LJ. Resolving páramo *Poa* (Poaceae): morphometric and phylogenetic analysis of the 'Cucullata complex' of north-west South America. Bot J Linn Soc. 2021;197: 104–146.

Trapnell C, Roberts A, Goff L, Pertea G, Kim D, Kelley DR, Pimentel H, Salzberg SL, Rinn JL, Pachter L. Differential gene and transcript expression analysis of RNA-seq experiments with TopHat and Cufflinks. Nat Protocols. 2012;7:562–578.

Van der Auwera GA, O'Connor BD. Genomics in the Cloud: using Docker, GATK, and WDL in Terra. Beijing: O'Reilly Media, Incorporated; 2020.

van der Valk T, Pečnerová P, Díez-del Molino D, Bergström A, Oppenheimer J, Hartmann S, Xenikoudakis G, Thomas JA, Dehasque M, Sağlıcan E, *et al.* Million-year-old DNA sheds light on the genomic history of mammoths. Nature. 2021;591: 265–269.

Venturini L, Caim S, Kaithakottil GG, Mapleson DL, Swarbreck D. Leveraging multiple transcriptome assembly methods for improved gene structure annotation. GigaScience. 2018;7:giy093.

Wang L-G, Lam TT-Y, Xu S, Dai Z, Zhou L, Feng T, Guo P, Dunn CW, Jones BR, Bradley T, *et al.* Treeio: an R package for phylogenetic tree input and output with richly annotated and associated data. Mol Biol Evol. 2020;37:599–603.

Wickham H. ggplot2: elegant graphics for data analysis. New York: Springer-Verlag; 2016.

Yu G. Using ggtree to visualize data on tree-like structures. Curr Protoc Bioinform. 2020;69:e96.

Zhang R-G, Wang Z-X, Ou S, Li G-Y. TEsorter: lineage-level classification of transposable elements using conserved protein domains. bioRxiv; 2019.

Editor: E. Akhunov